

Effect of Slope Geometries on 3D Slope Stability under the Influence of Infiltration

M S K Hassan*, V H Loo

Department of Civil and Construction Engineering, Curtin University Malaysia; CDT 250, 98009 Miri, Sarawak, Malaysia

*Corresponding author

doi: <https://doi.org/10.21467/proceedings.133.5>

ABSTRACT

Rainfall-induced slope failure is the most common type of slope failure in Malaysia. Many studies have been carried out to assess the correlation of infiltration to 2D geometric features such as slope inclination. However, the relationship between infiltration and 3D slope geometric features has not yet been widely studied. The aim of this study is to assess the effect of varying slope geometries on slope stability with the influence of rainfall, and to compare the results of the 2D and 3D slope analysis. Seepage and slope stability analysis of homogenous slopes for normal, curved surface and turning corner slopes of varying angles were modelled using the numerical software PLAXIS LE. The 3D analysis demonstrated that multiple shallow failures spread across the sloped surface, which could not be captured by the 2D analysis. The failure modes are similar for the various geometric types of slopes. The results also indicate that the safety factor from the 3D analysis decreases more significantly with the rainfall duration as compared to the 2D analysis. This study changes the perception that a 2D analysis is more conservative than a 3D analysis, which is not always true.

Keywords: Slope Stability, Infiltration, Slope Geometries

1 Introduction

Rainfall-induced slope failure is a common type of slope failure that occurs frequently in tropical regions such as East Malaysia, where the annual rainfall ranges from 3300 mm to 4600 mm (Sarawak Government 2021). Slope failures pose a considerable threat to human beings in the surrounding vicinity and cause damages to infrastructure, which result in severe economic losses. Global warming has led to an increase in the frequency and intensity of rainfall events (Huggel et al. 2013) and a surge in the extreme rainfall event conditions (Hausfather 2018). Figure 1 illustrates the variation of the average global temperature and precipitation with their respective trends over the last 120 years (NASA/GISS 2019). The increase in precipitation has caused a rise in the number of annual landslide occurrences (Petley 2012). Therefore, this is a concern as landslides will only increase with time and hence, it must be diligently investigated.

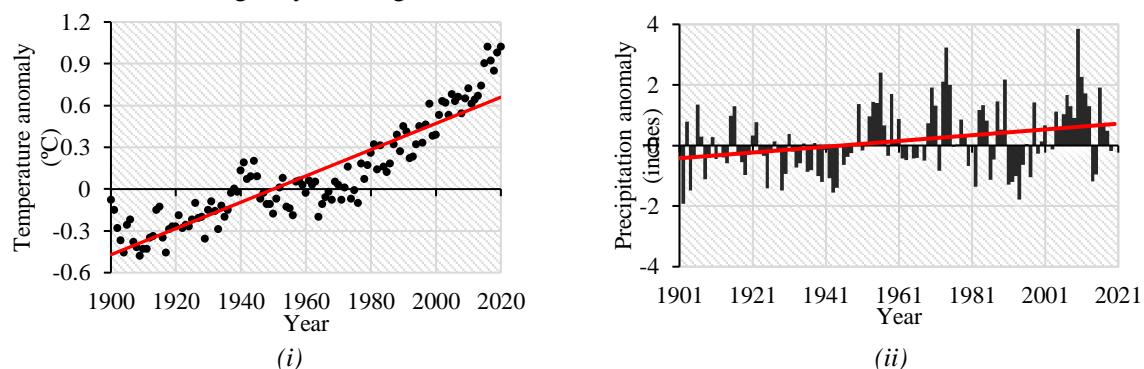


Figure 1:(i) Average global temperature change and (ii) Average global precipitation change (NASA/GISS 2019)



© 2022 Copyright held by the author(s). Published by AIJR Publisher in the "Proceedings of The HKIE Geotechnical Division 42nd Annual Seminar: A New Era of Metropolis and Infrastructure Developments in Hong Kong, Challenges and Opportunities to Geotechnical Engineering" (GDAS2022) May 13, 2022. Organized by the Geotechnical Division, The Hong Kong Institution of Engineers.

Intensity of rainfall is one of the major factors that affects the stability of the slope. The study carried out by Gasmu, Rahardjo, and Leong (2000) showed that a rainfall event with an intensity of approximately 16 mm/hr would decrease the factor of safety (FoS) by around 10%, while the rainfall intensity of 55 mm/hr would cause a decrease of around 25%. This highlights that an increase in the rainfall intensity has a detrimental effect on the factor of safety. This finding is in line with the study carried out by researchers such as Hossain, Hossain, and Hoyos (2013) and Kristo, Rahardjo, and Satyanaga (2017). It is anticipated that the increase of rainfall intensity would induce more severe slope failures.

Another key characteristic that influences slope stability is the geometry of the slope. Several studies on two-dimensional (2D) slope geometries have been conducted to investigate the effect of slope angle on the stability of the slope (Zakaria et al. 2018; Chatterjee and Murali Krishna 2019; Zhou et al. 2020). In addition, Chatterjee and Murali Krishna (2019) investigated the correlation of 2D slope geometries with infiltration. Their results indicate that an increase in slope angle would decrease the amount of infiltration into the sloped surface, thus reducing the decrease in the FoS during the rainfall event.

Three-dimensional (3D) slope geometric features such as curved surfaces, turning corners, etc can be observed in several man-made slopes in slope engineering, road engineering, etc. Examples of these features have been illustrated in Figure 2. The study carried out by Zhang et al. (2013) showed that these geometrical features can influence the FoS by as much as 20% and affect the failure surface. Based on the literature review, it has been identified that a majority of the studies focused on 2D slope geometry but the correlation between 3D geometric features and infiltration has not yet been well-studied.



Figure 2: Example of (i) curved surfaced slopes at Canada Hill at Miri, Sarawak and (ii) turning corner slopes (Call and Nicholas 2021)

In current industrial practices, running a 3D analysis is not compulsory on the account that a 2D analysis will generally lead to a conservative result, of which the most critical 2D cross-section is identified and analysed. However, studies indicate that a 2D analysis could lead to an inadequate representation of the conditions of slope failures (Stark and Eid 1998; Chaudhary, Fredlund, and Lu 2016). This is because a 2D analysis assumes plane strain conditions and hence, it does not consider the effects of 3D geometry such as convex and concave configurations. Therefore, the actual extent of the failure surface and volume cannot be captured. The understanding that FoS_{3D} is higher than FoS_{2D} is based on research that has not considered the factor of seepage due to rainfall.

Over the last decade, the commercially available 3D slope stability analysis software and advancement in computing technology has seen a major development. Therefore, running a 3D analysis has become affordable as it is cost and time efficient. The objective of this study is to assess the effect of varying 3D slope geometries on slope stability by the influence of rainfall, and to compare the results of the 2D and 3D slope analysis. Three slope geometries: normal, curved surface and turning corner slopes of varying angles were modelled. The following sections will introduce the method used and discuss the results obtained.

2 Material and Methods

The analyses were carried out using the Groundwater and Slope Stability modules of PLAXIS LE by Bentley Systems (Bentley Systems 2022). A seepage analysis was first carried out to obtain the pore pressure distribution, followed by a slope stability analysis to assess the factor of safety of the slope. The methodology can be classified into three stages. The first stage is to validate the model to ensure the ability to perform the required tasks with acceptable accuracy. The second stage involves an analysis of a 3D idealized slope with and without rainfall infiltration. The final stage involves a comparative analysis where 2D slices of the 3D models were extracted and analysed, subjected to the same conditions as the 3D models.

2.1 Validation

A case study by Fredlund, Rahardjo, and Fredlund (2012) was selected to validate the seepage flow of the model. This case was tested and verified experimentally and numerically by the original authors and hence, is of high value for validation purposes. The case involves a 2D multi-layered slope subjected to a constant rainfall flux of 756 mm/hr into the slope. Surface runoff was not considered in the model. A transient analysis with a total duration of 280 seconds was carried out. The total head contours at various timesteps were compared with the original results and identical results were obtained with only minor discrepancies. Figure 3 illustrates a sample of the original and obtained result.

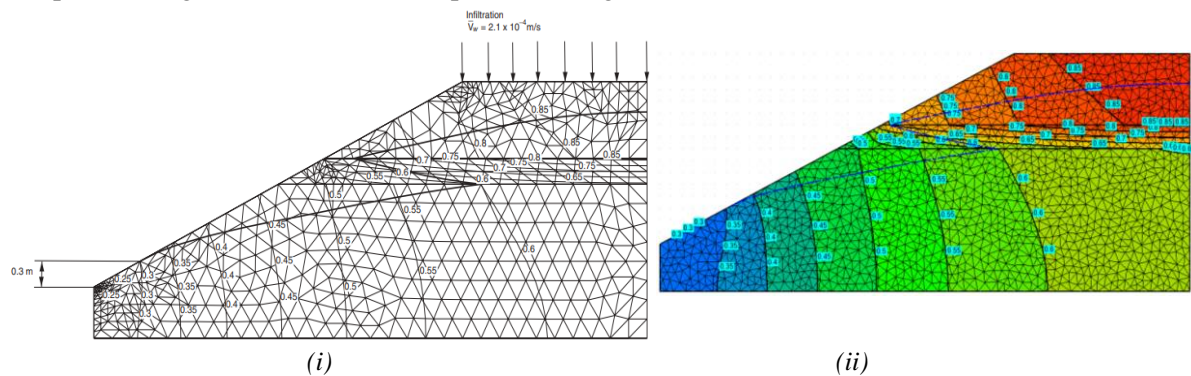


Figure 3: (i) Original seepage result at $t = 260s$ (Fredlund, Rahardjo, and Fredlund 2012) and (ii) recreated seepage model

To test the slope stability module, a case study by Leong and Rahardjo (2012) has been selected. The case involves a 3D, single-layered slope overlying bedrock with the water table at the ground surface. An effective stress analysis with varying shear strength parameters was conducted and the soil shear strength was modelled using the Mohr-Coulomb failure criterion. Some of the FoS results have been listed in Table 1 below. The obtained failure surface was comparable to the original result. The accuracy of the validation results obtained from both analyses were acceptable.

Table 1: Comparison of the FoS results of validated model and the case studies

Soil Parameters		Factor of safety (method of analysis)		
Effective friction angle	Effective cohesion	Bishop*	Morgenstern and Price*	Current Study (Morgenstern and Price)
32.0	2.0	0.560	0.660	0.603
32.0	10.6	0.895	0.908	0.942
36.4	10.6	0.990	1.006	1.051

* Represents results taken from Leong and Rahardjo (2012)

2.2 Slope Geometrical Variants

The three types of varying 3D slope geometries include normal, curved surfaces and turning corners. The slope inclination is 45 degrees for all the types. The geometries will be further elaborated in the following paragraphs.

Type 1 is the normal slope. Figures 4 (i) and 4 (ii) illustrate the cross section in 2D (with dimensions in meters) and 3D, respectively. The length and width of the slope was taken as 180 m and 120 m, respectively.

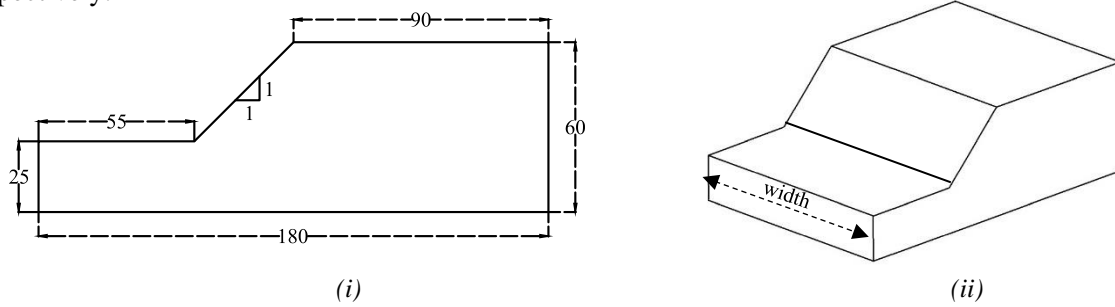


Figure 4: (i) Cross-sectional view and (ii) 3D view of normal slope

Type 2 is the curved surface slope. Concave and convex curved surface slopes of various curvatures were modelled. The degree of curvature was expressed by the parameter R_{cur} (Zhang et al. 2013) as shown in the following formula:

$$R_{cur} = \frac{L}{W} \tag{1}$$

In equation (1), L is the distance that the sloped surface bulges in (concave) or out (convex) at the toe and crest, and W is the width of the slope which is 120m. The slope retains the same cross-sectional dimensions illustrated in Figure 4. Figure 5 illustrates an example of a concave curved surface slope, convex curved surface and a 3D model of a concaved slope surface. The annotations A, B and C represent the region behind the crest of the slope, the region in front of the slope toe and the sloped surface, respectively. Table 2 (second row) summarizes all the curved surface slope variants that were included in the analysis. The negative values in the table refer to curved surfaces that are in the outward direction.

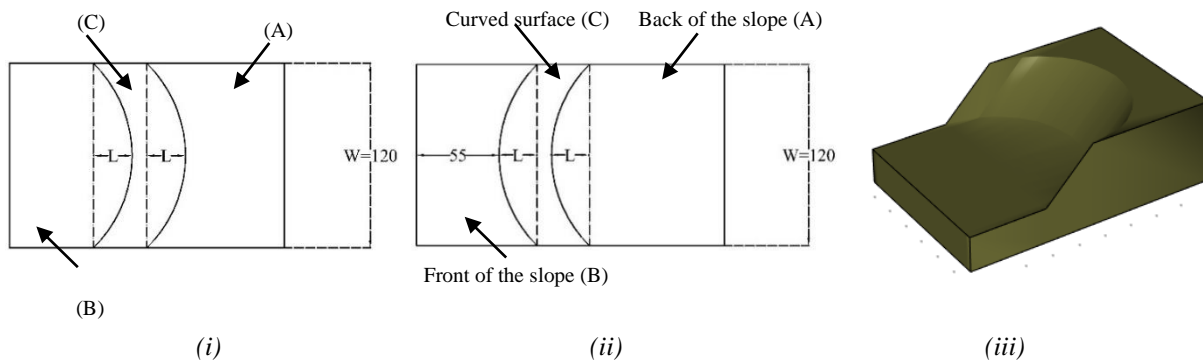


Figure 5: Plan view of (i) concave, (ii) convex and (iii) 3D concave curved surface slope

Type 3 is the turning corner slope. The turning corner angle (α) is measured from the outside of the slope as displayed in Figure 6. The slope retains the same cross-sectional dimensions as illustrated in Figure 4. Table 2 (third row) summarizes all the variants that were included in the analysis.

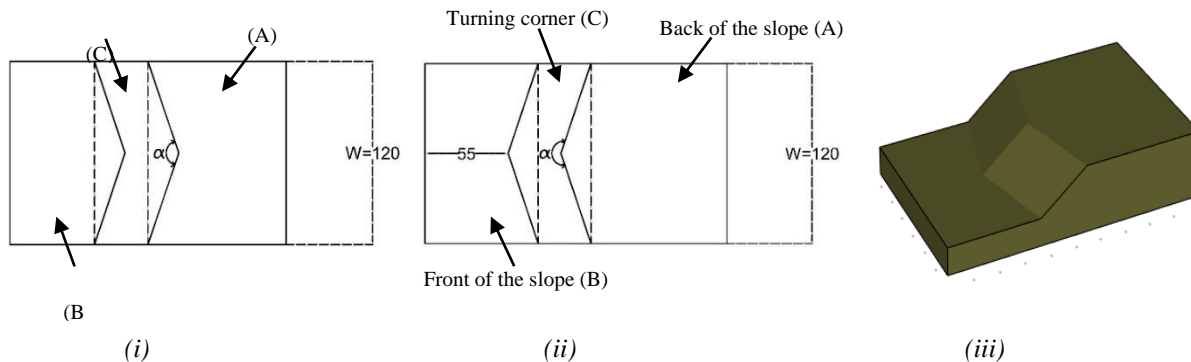


Figure 6: Plan view of (i) concave, (ii) convex and (iii) 3D convex turning corner slope

Table 2: Curved surface and turning arc slope variants

Geometrical variant type	Shape parameter	Concave			Normal	Convex		
		3/6	2/6	1/6	0	-1/6	-2/6	-3/6
Curved surface slope (ref. Figure 5)	R_{cur}	3/6	2/6	1/6	0	-1/6	-2/6	-3/6
Turning corner slope (ref. Figure 6)	α	90°	120°	150°	180°	210°	240°	270°

2.3 Seepage Analysis

The Groundwater module of PLAXIS LE is a finite element (FEM) analysis software that has been used for the seepage analysis.

2.3.1 Hydraulic Soil Properties

The study adopted the soil properties of sand from West Malaysia referring to research from Gofar and Lee (2008). Table 3 lists the hydraulic properties of soil. The soil water characteristic curve (SWCC) and permeability function curves were based on the van Genuchten (1980) model as illustrated in Figure 7.

Table 3: Hydraulic properties of sand soil (Gofar and Lee 2008)

Soil parameters	Symbol	Value	Unit
Saturated volumetric water content	w_s	0.450	-
Saturated permeability	k_s	3.4×10^{-4}	m/s

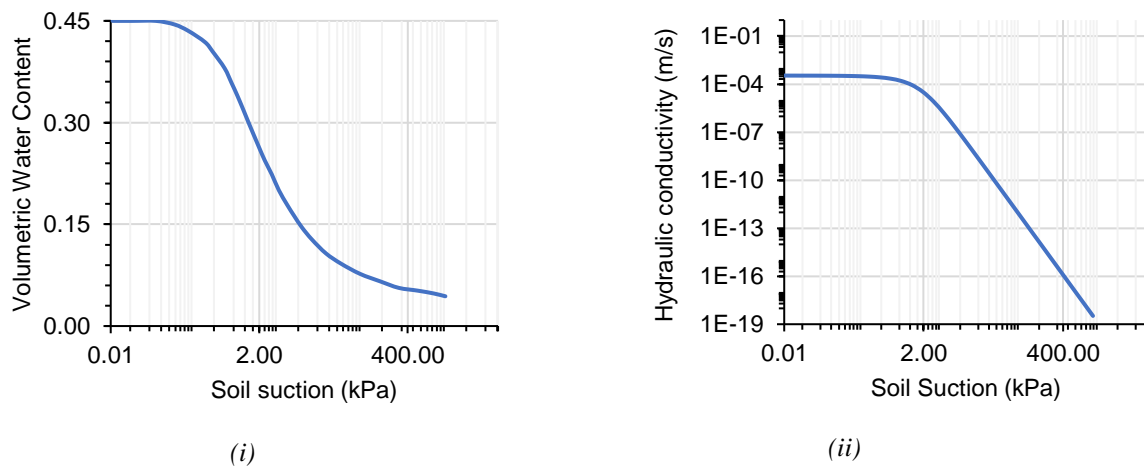


Figure 7: Recreated (i) SWCC and (ii) permeability function curve of the sand soil (Gofar and Lee 2008)

2.3.2 Hydraulic Boundary Conditions

Figure 8 illustrates the seepage model of the 2D and 3D normal slope. The initial water table was set at the mid heights of each of the sides, in which a constant head (A) was applied below the water table at both side regions of the slope. The side regions above the water table were set to zero nodal flux (B). To model rainfall, a vertical flux (C) with a constant intensity of 35 mm/hr for a total duration of 6 hours was applied to the ground surface.

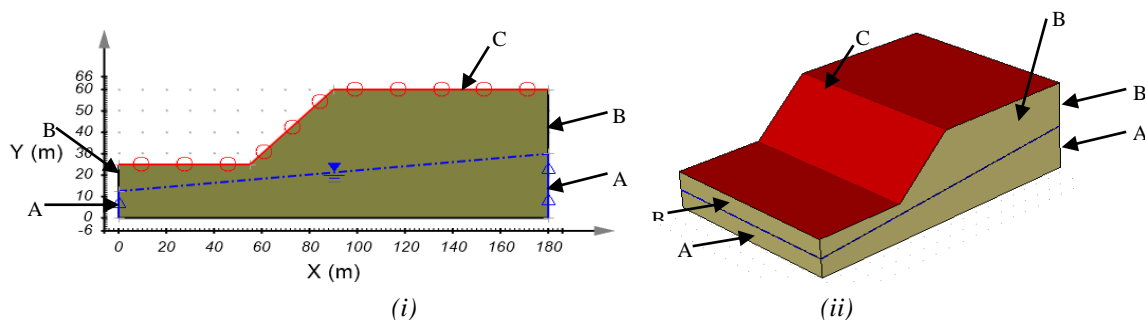


Figure 8 Hydraulic boundary conditions for (i) 2D normal slope and (ii) 3D normal slope

2.4 Slope Stability Analysis

The Slope Stability module of PLAXIS LE is a limit equilibrium (LEM) analysis software under Bentley systems. The linear Phi-b model (Bentley Systems 2020) enables the modelling of unsaturated shear strength taking into account the matric suction and has been adopted for this study.

2.4.1 Mechanical and Material Soil Properties

Table 4 lists the bulk unit weight and shear strength parameters used for the modelling, referring to the study by Gofar and Lee (2008).

Table 4: Soil mechanical and material properties based on Gofar and Lee (2008)

Parameter	Symbol	Value	Unit
Unit weight	γ	19.44	kN/m ³
Effective friction angle	ϕ'	35.0	°
Unsaturated friction angle	ϕ^b	14.0	°
Effective cohesion	c'	1.0	kN/m ²

2.4.2 Search Method for Critical Slip Surface and Calculation Methods

The most critical failure surface was identified through a trial-and-error slip search process known as the grid and tangent method, which assumes circular failure surfaces. For each 3D analysis, over 103,000 trial surfaces were analysed, while for the 2D analysis, over 1500 surfaces were evaluated. For the calculation method, the Morgenstern and Price’s method, which satisfies both the force and moment equilibrium equations, was used. Morgenstern and Price’s method assumes that the interslice shear forces are a function of normal forces. The half-sine function, which has been commonly used Rawat and Gupta (2016) and Beyene (2017) was adopted.

3 Results and Discussion

3.1 Distribution of Pore Pressure

Figure 9 illustrates a comparison of the 3D (elevation view) and 2D normal slope seepage analysis result at the 0-hr and 6-hr rainfall duration. For the 2D results, it was observed that with the duration of the rainfall, there is a decrease in the matric suction near the sloped surface (annotation A on Figure 9 (iii) and (iv)). This is because as rainfall infiltrates the soil, the volumetric water content increases which results in a decrease in the matric suction as illustrated in Figure 7 (i). In addition to this, the water table rose minorly (yellow line indicated by annotation B in Figure 9 (iii) and (iv)) and the formation of the wetting front at the sloped surface was observed (yellow line indicated by annotation C in Figure 9 (iii)). These findings are in line with the 3D seepage results. These observations are common for all the geometric variants.

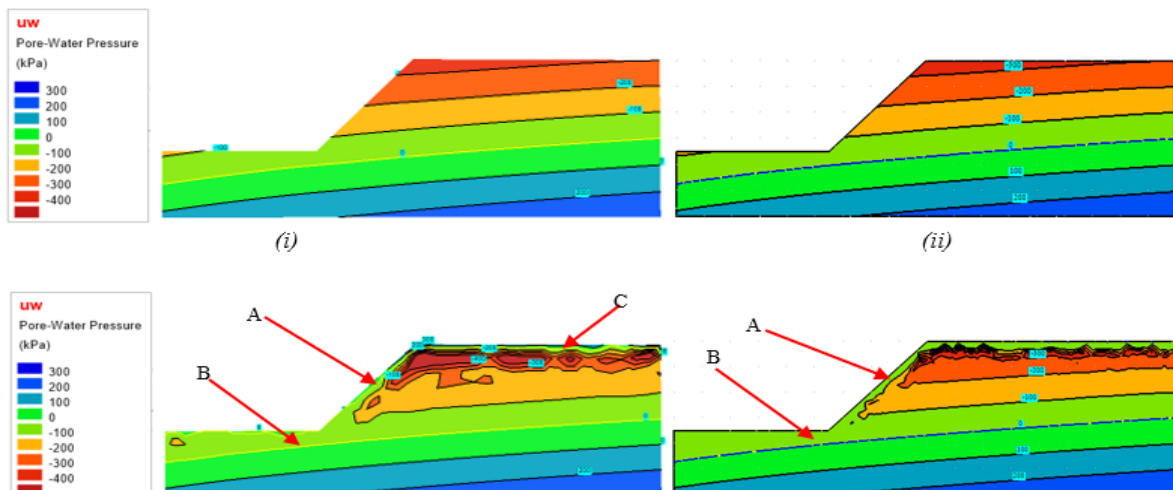


Figure 9: Pore pressure distribution of the (i) 0-hr timestep for the 3D (elevation view) normal slope, (ii) 0-hr timestep for the 2D normal slope, (iii) 6-hr timestep for the 3D (elevation view) normal slope and (iv) 6-hr timestep for the 2D normal slope

3.2 Comparison of Failure Surfaces When Utilizing a 3D Analysis Over a 2D Analysis

Figure 10 demonstrates a comparison of the slope stability results at the 1.5-hr and 6-hr rainfall duration for the 3D and 2D normal slope. Initially, the FoS of both 3D and 2D results are similar and their critical slip surfaces behave as a global failure (Figures 10 (i) and (iii)). However, with the rainfall infiltration, the slip surface becomes localized and shallow for both cases. The 3D results show numerous shallow failure surfaces (FoS < 1) spreading throughout the sloped surfaces (critical slip surface for the 3D model has been marked in black in Figure 10 (ii)).

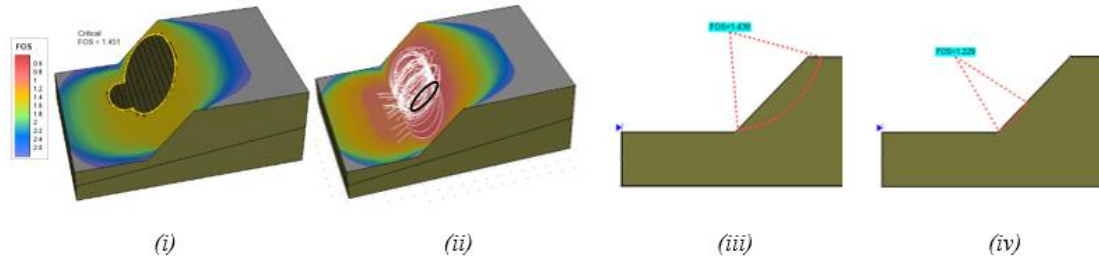


Figure 10: Failure surface for the 3D normal slope at (i) 1.5-hr and (ii) 6-hr, and the 2D model at (iii) 1.5-hr and (iv) 6-hr

Figure 11 displays an example of the spread of the failures with the duration of rainfall for a 3D curved surface slope. Similar to the 2D models, the slope initially experiences a global failure. However, as the rainfall event progresses, instead of a single slip surface, the result demonstrates several shallow failures (FoS < 1) spreading across the sloped surface (critical slip surface has been marked in black in Figures 11 (ii) and (iii)). This is due to the continuous decrease in matric suction as the rainfall duration increases. The normal, curved surface and turning corner slopes exhibited identical features. This result is significant as it highlights that a 3D analysis is able to detect the spread of multiple shallow failures.

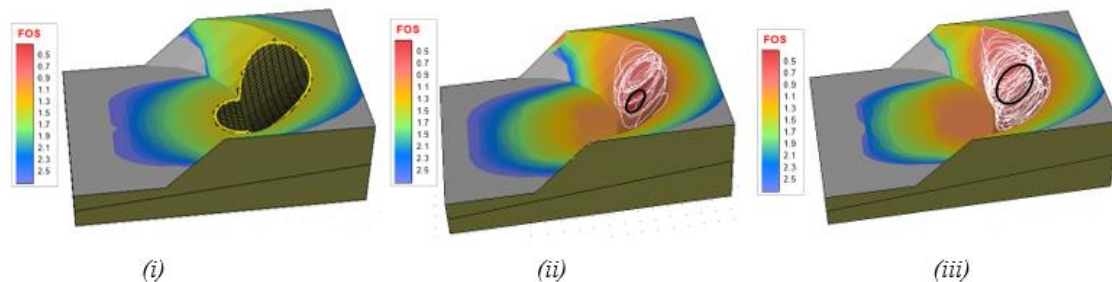


Figure 11: Failure surfaces (FoS < 1) for concave curved surface with $R_{cur} = 3/6$ at (i) 1.5-hr, (ii) 4.5-hr and (iii) 6-hr

The failure surface for the turning corner slopes was unique where the failure surfaces varied with change in the turning corner angle. Figures 12 (i) and (ii) demonstrate that for concave turning corner slopes of decreasing turning angle, the failures were spread across both sides of the slope. Conversely, Figures 12 (iii) and (iv) illustrate that for convex turning corners of increasing turning angle, the failures were concentrated at the ridge of the slope (critical slip surface has been marked in black in Figure 12). A potential cause for this observation is that a higher concentration of positive pore pressures is distributed near the ridge of the slope for the convex variants than the concave variants, resulting in a narrow extent of slope failures at the ridge of the slope. This demonstrates how the geometry of the slope will affect the distribution of rainfall as well as the distribution of slope failure surfaces. This finding could not have been observed from a 2D analysis as it assumes plane strain conditions.

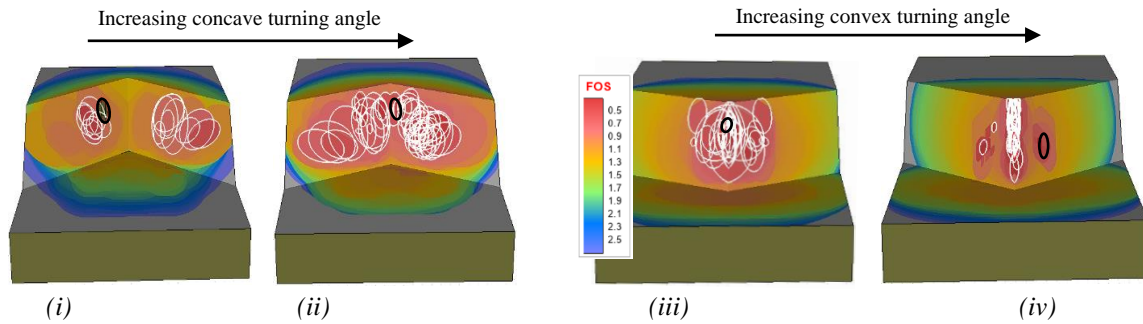


Figure 12: Spread of failures of slip surfaces (FoS<1) for turning corner slopes at the 6-hr duration for (i) concave 90, (ii) concave 120, (iii) convex 240 and (iv) convex 270

3.3 Changes of FoS for 3D Analysis

For the models in which multiple shallow failures were observed, the 10 most critical failures were selected to evaluate the FoS of the slope. The range of the critical FoS values for these models were considered using range bars in the graph with the average critical FoS represented by the points in the graph. The type of turning corner has been selected to illustrate the changes of FoS with the duration of the rainfall event as illustrated in Figure 13. It is observed that the FoS decreases nonlinearly as the rainfall event progresses. This is due to the decrease in the shear strength that occurs due to the decrease in the matric suction. A greater decrease in the FoS for convex variants when compared to the concave variants was also observed. This is potentially because the convex slopes have a greater surface area behind the slope crest when compared to the concave counterparts, giving a larger area of infiltration for the convex slopes. These findings are common amongst all the geometric variants.

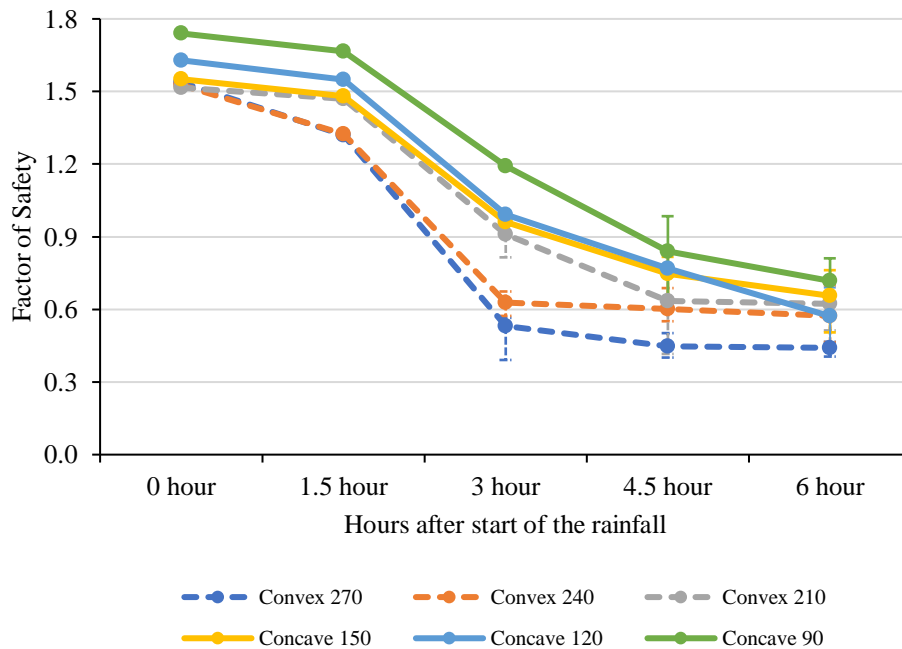


Figure 13: Variation of the factor of safety for the turning corner slopes

3.4 Changes of FoS for 3D Analysis and 2D Analysis

To illustrate the comparison between the 2D and 3D analysis results, a single case has been selected from each geometric variant type. The results have been plotted in Figure 14. The changes in the FoS for 2D analysis is much more gradual compared to the 3D analysis. The FoS for the critical slip surface of the 3D analysis decreases by around 51%, 54% and 71% for the normal, curved surface and turning corner slope, respectively. However, the FoS decrease for the 2D analysis is only around 16%, 17% and 11% for the normal, curved surface and turning corner slope respectively. As the rainfall event

progresses, the FoS of the 3D results are below 1 but the FoS of 2D results are still above 1. While the conservative 3D results were observed for failures that are shallow in depth and small in volume, it is nonetheless a substantial finding as it changes the perception of our common understanding that a 2D slope stability analysis will always yield a conservative result when compared to a 3D analysis. The 3D analysis enables the distribution of pore water in 3 dimensions, which increases various potential failure surfaces of slope. The trend in the change of the FoS for the other models are similar.

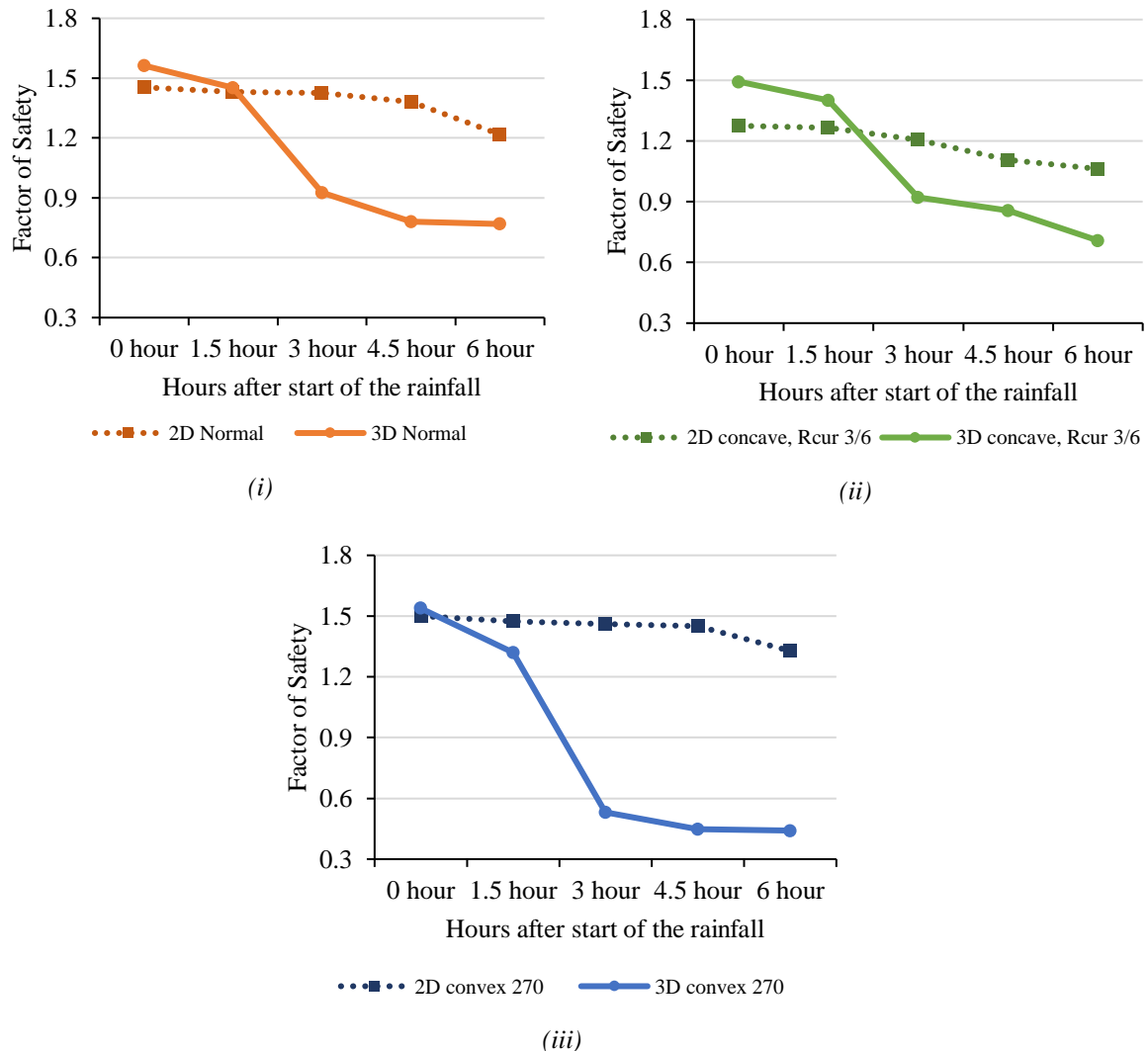


Figure 14: Comparison of the factor of safety for the (i) 2D and 3D normal slope, (ii) 2D and 3D concave R_{cur} 3/6 curved surface slope and (iii) 2D and 3D concave 270 turning corner slope

4 Conclusions

Rainfall-induced slope failure is the most common type of slope failure in Malaysia. In the past, most of the studies' focus on rainfall-induced slope failures are in 2D analysis. The influence of rainfall to the 3D geometric features has not yet been well-studied. The objective of this study is to evaluate the effect of utilizing a 3D analysis over a 2D analysis for slopes of varying geometry subjected to rainfall. Homogenous sandy slopes with a 1:1 (horizontal to vertical) slope inclination was modelled using the numerical software PLAXIS LE. A seepage analysis was carried out to obtain the pore pressure distribution for a specific rainfall event. The slope stability analysis was then assessed using Morgenstern and Price's limit equilibrium method. During rainfall, for all slope geometries, the 3D analysis indicated that several shallow failures occur across the sloped surfaces. Similar trends in the decrease of the FoS with the duration of the rainfall were observed for slope geometries such as the normal, curved surface and turning corner slopes. When comparing the 2D and 3D analysis results without rainfall, the FoS from the 2D analysis is generally lower. However, the FoS from the 3D analysis decreases more significantly as the rainfall event progresses while the FoS from the 2D analysis

decreases gradually. Hence, resulting in a conservative result from the 3D analysis. This study demonstrated that a 3D analysis is advantageous to capture shallow and localized slope failures spreading across the sloped surface. This study gives new insights of understanding slope failures under the influence of rainfall, which ultimately highlights the fact that running a 3D seepage and slope stability analysis is of paramount importance. Furthermore, affordable computing technology has become more accessible over the last decade and is continuing to advance even now. Therefore, running a 3D analysis should be encouraged amongst the engineers to provide a more sustainable and cost-effective design in the industry.

5 Declarations

5.1 Acknowledgements

This research was supported under the budget for final year projects by Faculty of Engineering and Science, Curtin University Malaysia. The authors would also like to thank Ir. Dr. Wong Kwong Soon, the unit leader, and the lecturers Dr. Tang Fu Ee and Dr. Yong Leong Kong for their constructive comments during the proposal and final presentation. The authors would also like to express gratitude towards Dr. Choo Chung Siung of Swinburne University for his comments during the final presentation. Also, special thanks to Mr. Sheikh Zaffrullah, who aided in providing technical support.

5.2 Publisher's Note

AIJR remains neutral with regard to jurisdictional claims in published maps and institutional affiliations.

References

- Bentley Systems. 2020. SVSLOPE 2D/3D limit equilibrium slope stability analysis - Theory manual. 1–235.
- Bentley Systems. 2022. PLAXIS LE - Limit equilibrium geotechnical application. <https://www.bentley.com/en/products/product-line/geotechnical-engineering-software/plaxis-le>.
- Call and Nicholas. 2021. Open Pit Mining Geotechnical Consulting Services - Call & Nicholas, Inc. 2021. <https://www.cnitucson.com/openpit.html>.
- Chatterjee, D. & Murali Krishan, A. 2019. Effect of slope angle on the stability of a slope under rainfall infiltration. *Indian geotechnical journal*, 49(6): 708–17. <https://doi.org/10.1007/s40098-019-00362-w>.
- Chaudhary, K.B., Fredlund, M. & Lu, H. 2016. Three-dimensional slope stability: Geometry effects. In *Tailings and mine waste '16*. Colorado.
- Fredlund, D. G., Rahardjo, H. & Fredlund, M.D. 2012. *Unsaturated soil mechanics in engineering practice*. John Wiley & Sons, Inc. <https://doi.org/10.1002/9781118280492>.
- Gasmo, J. M., Rahardjo, H. & Leong, E.C. 2000. Infiltration effects on stability of a residual soil slope. *Computers and Geotechnics*, 26(2): 145–65. [https://doi.org/10.1016/S0266-352X\(99\)00035-X](https://doi.org/10.1016/S0266-352X(99)00035-X).
- Genuchten, M. Th. van. 1980. A closed-form equation for predicting the hydraulic conductivity of unsaturated soils. *Soil science society of America journal*, 44(5): 892–98. <https://doi.org/10.2136/sssaj1980.03615995004400050002x>.
- Gofar, N. & Lee, M.L. 2008. Extreme rainfall characteristics for surface slope stability in the Malaysian peninsular. *Georisk*, 2(2): 65–78. <https://doi.org/10.1080/17499510802072991>.
- Hossain, J., Hossain, M.S. & Hoyos, L. R. 2013. Effect of rainfall on stability of unsaturated earth slopes constructed on expansive clay. In *Geo-Congress 2013: Stability and Performance of Slopes and Embankments III*, 417–25. American Society of Civil Engineers (ASCE). <https://doi.org/10.1061/9780784412787.042>.
- Huggel, C., Khabarov, N., Korup, O. & Obersteiner, M. 2013. Physical impacts of climate change on landslide occurrence and related adaptation. In *Landslides*, 121–33. Cambridge University Press. <https://doi.org/10.1017/cbo9780511740367.012>.
- Leong, E. C. & Rahardjo, H. 2012. Two and three-dimensional slope stability reanalyses of bukit batok slope. *Computers and geotechnics*, 42: 81–88. <https://doi.org/10.1016/j.compgeo.2012.01.001>.
- NASA/GISS. 2019. Global temperature | Vital signs – climate change: vital signs of the planet. <https://climate.nasa.gov/vital-signs/global-temperature/>.
- Petley, D. 2012. Global patterns of loss of life from landslides. *Geology*, 40(10): 927–30. <https://doi.org/10.1130/G33217.1>.
- Sarawak Government. 2021. Geography. [sarawak.gov.my. https://sarawak.gov.my/web/home/article_view/159/176/?id=159](https://sarawak.gov.my/web/home/article_view/159/176/?id=159).
- Singh, R., Umrao, R.K. & Singh, T.N. 2017. Hill slope stability analysis using two and three dimensions analysis: A comparative study. *Journal of the geological society of India*, 89(3): 295–302.

- <https://doi.org/10.1007/s12594-017-0602-2>.
- Stark, Timothy D. & Hisham T. Eid. 1998. Performance of Three-Dimensional Slope Stability Methods in Practice. *Journal of Geotechnical and Geoenvironmental Engineering* 124 (11): 1049–60. [https://doi.org/10.1061/\(asce\)1090-0241\(1998\)124:11\(1049\)](https://doi.org/10.1061/(asce)1090-0241(1998)124:11(1049)).
- Zakaria, Z., Sophian, I., Sabila, Z.S. & Jihadi, L. H. 2018. Slope safety factor and its relationship with angle of slope gradient to support landslide mitigation at Jatinangor education area, Sumedang, West Java, Indonesia.” *IOP conference series: Earth and environmental science*, 145(1): 0–8. <https://doi.org/10.1088/1755-1315/145/1/012052>.
- Hausfather, Z. 2018. Explainer: What Climate models tell us about future rainfall. *Carbon brief*. <https://www.carbonbrief.org/explainer-what-climate-models-tell-us-about-future-rainfall>.
- Zhang, Y., Chen, G., Zheng, L., Li, Y. & Zhuang, X. 2013. Effects of geometries on three-dimensional slope stability. *Canadian geotechnical journal*, 50(3): 233–49. <https://doi.org/10.1139/cgj-2012-0279>.
- Zhou, Y., Qi, S.C., Fan, G., Chen, M.L. & Zhou, J.W. 2020. Topographic effects on three-dimensional slope stability for fluctuating water conditions using numerical analysis. *Water (Switzerland)*, 12(2): 615. <https://doi.org/10.3390/w12020615>.